Supplementary Figures 1, 2, 3

Morphology of the zircons

Cathodoluminescence (CL) images of the selected zircons analyzed by SHRIMP II are shown in Supplementary Figures 1, 2, 3. Circles indicate location of analytical spots, where spot number and age with 1σ error are shown. Rhyolites XL31 and XL34 from the lower unit of the Xinglonggou lavas are dominated by euhedral needle shaped zircons with oscillatory (Supplementary Figure 1A, C, D, E and Supplementary Figure 2B, C, E, F) to banded (Supplementary Figure 1B, F and Supplementary Figure 2A, D) zoning, which agree with a volcanic origin of rapid crystallization (Corfu *et al*., 2003). The volcanic zircons from the two samples show identical ages, with weighted mean $^{206}Pb/^{238}U$ ages of 159±3Myr (2σ, MSWD=1.01, 16 analyses) for XL 31 and 159±4Myr (MSWD=0.32, 16 analyses) for XL34 (Fig. 2a).

Like sample XL18 (Fig. 2b), high-Mg adakite XL03 from the upper unit of the Xinglonggou lava is dominated by sub-rounded inherited zircons which are mostly 2.4-2.5 Gyr (Supplementary Figure 3E, F; also see Fig. 2c). Inherited zircons of 2.0 Gyr and 840-950Myr (Supplementary Figure 3D; Fig. 2a, c) are also present. Note the sub-rounded form of inherited zircons (left inset of Fig 2b, Supplementary Figure 3F) with a very thin bright rim (Supplementary Figure 3E). Three small zircons (<50μm in diameter) of equant form and lacking internal structure (Supplementary Figure 3A, B) or weak, patchy structure (Supplementary Figure 3C) have ages of 141 to 149 Myr with weighted mean $^{206}Pb/^{238}U$ age of 144±9Myr (Fig. 2a). Two of them and one Neoproterozoic zircon were analyzed by SHRIMP II on the same spots (red circles in Supplementary Figure 3A, C, D) in the June 6.2002 session and the Dec.3-4.2003 session (Supplementary Table 1). Ages from the two sessions on the same three spots show good agreement with relative errors ranging from 0.78 to 4.4%. The three latest Jurassic zircons have Th/U ratios of 0.87 to 0.99 (Supplementary Table 1), typical of magmatic zircons. No Mesozoic granitoids and dykes are observed to intrude the Xinglonggou lava at the sampling area. Thus the latest Jurassic zircons are considered to represent the age of the upper unit of the Xinglonggou lavas.

Reference not cited in main paper

Corfu, F., Hanchar, J.M., Hoskin, P.O.W. & Kinny, P. Atlas of zircon textures. In *Zircon* (eds Hanchar, J. M. & Hoskin, P.W.O.) 469–500 (Reviews in Mineralogy & Geochemistry, Vol. 53, Mineralogical Society of America and Geochemical Society, 2003).

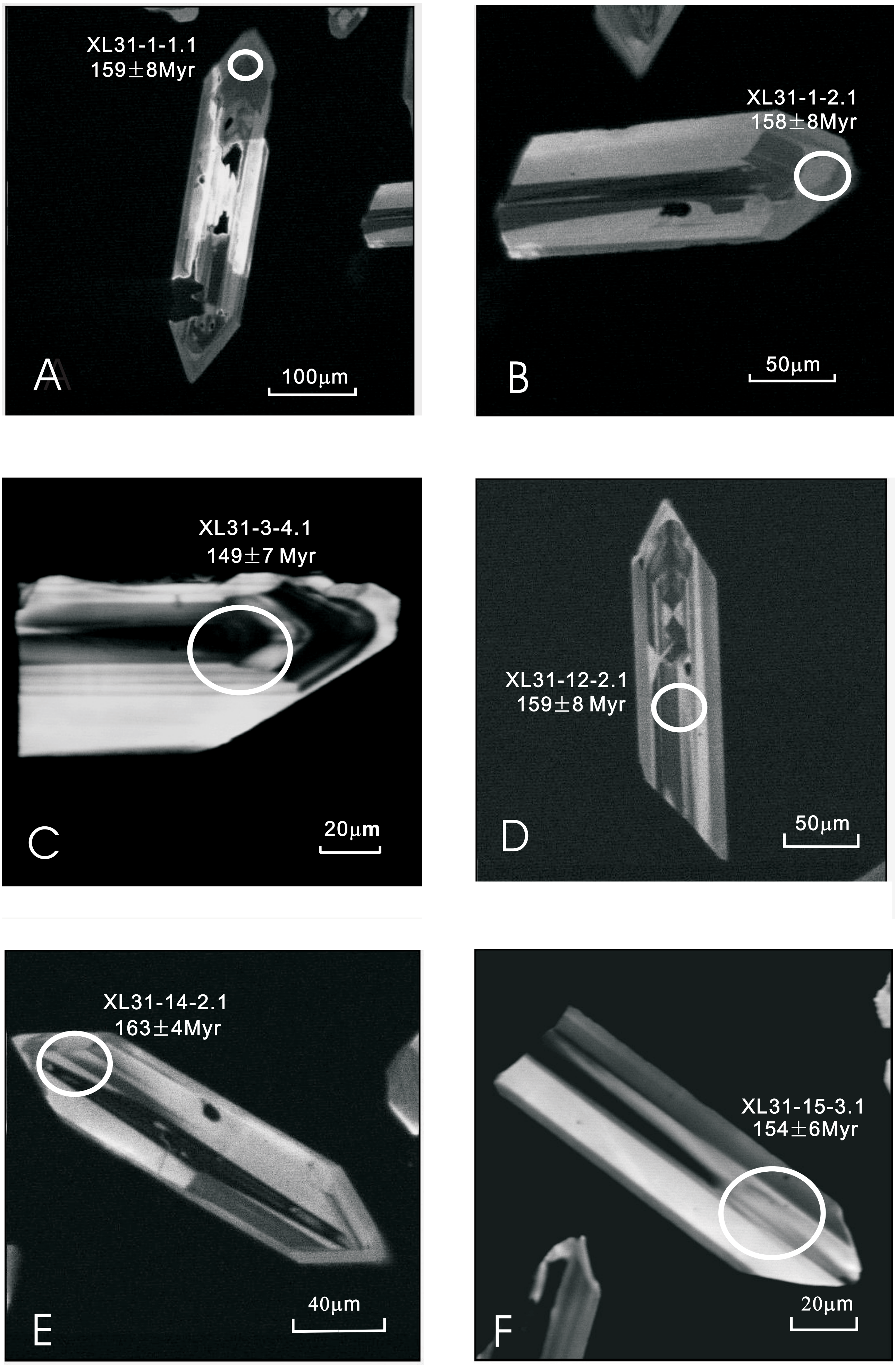

Supplementary Figure 1

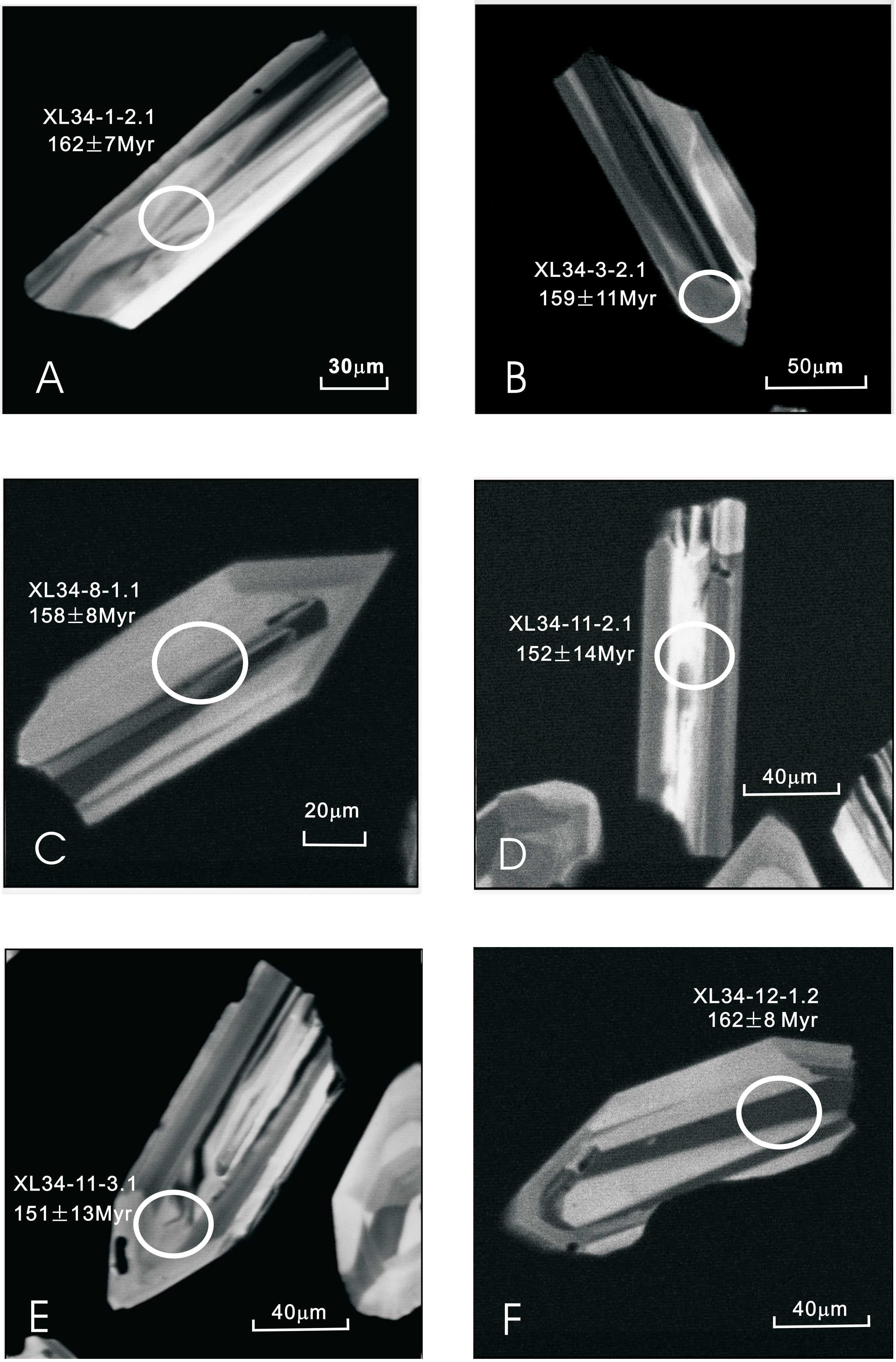

Supplementary Figure 2

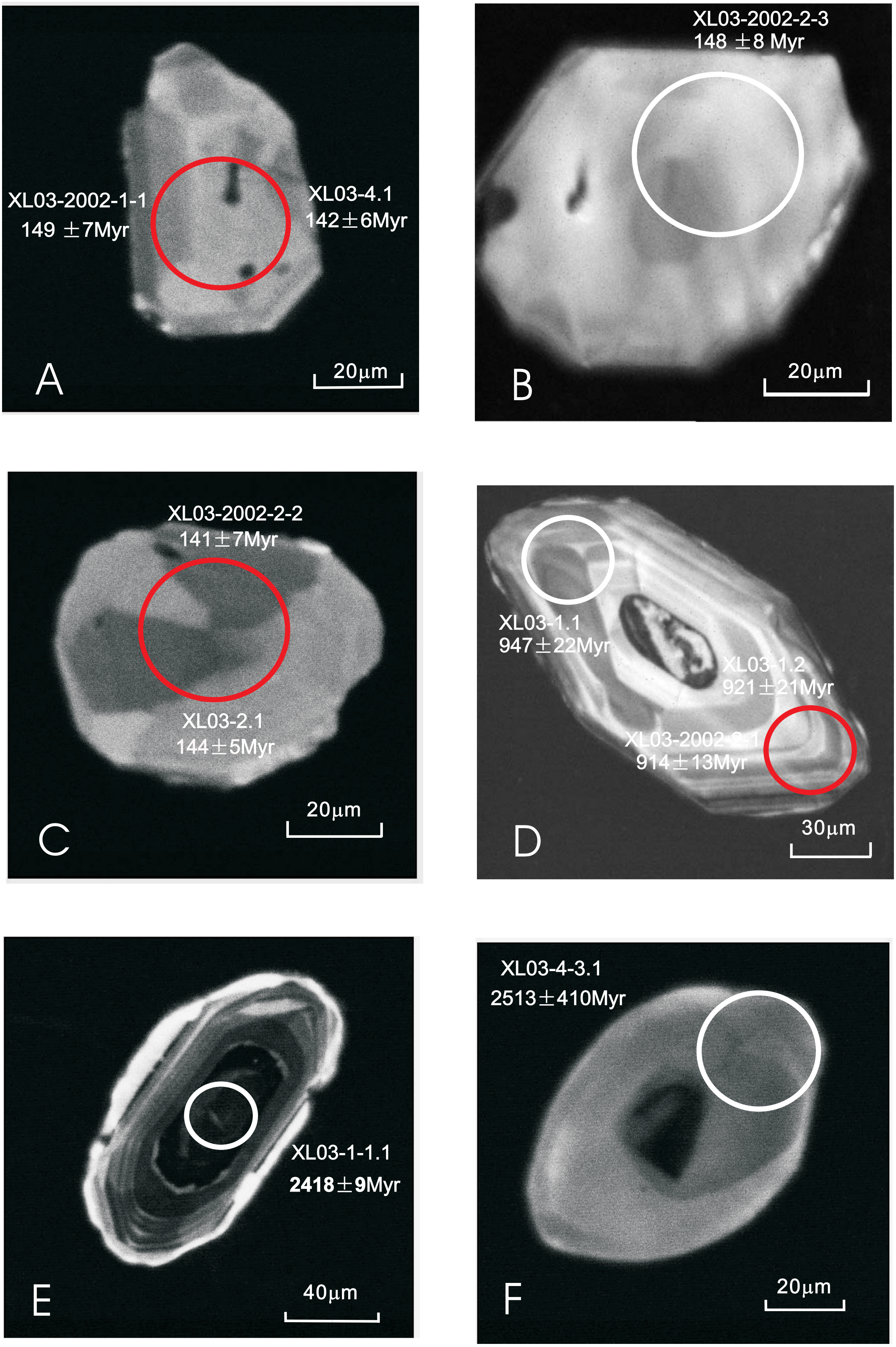

Supplementary Figure 3

Supplementary Data

Zircon $^{207}Pb/^{206}Pb$ ages of Archaean and Paleoproterozoic rocks from the North China Craton (Fig. 2c) are taken from the following sources.

Guan, H., Sun, M., Wilde, S.A., Zhou, X.H. & Zhai, M.G. SHRIMP U-Pb zircon geochronology of the Fuping Complex: implications for formation and assembly of the North China Craton. *Precambr. Res.***113**, 1–18 (2002).

Kröner, A., Cui, W.Y., Wang, W.Y., Wang, C.Q. & Nemchin, A.A. Single zircon ages from high-grade rocks of the Jianping Complex, Liaoning Province, NE China. *J. Asian Earth Sci*. **16**, 519–532 (1998).

Kröner, A., Wilde, S.A., Li, J.H. & Wang, K.Y. Age and evolution of a late Archean to Paleoproterozoic upper to lower crustal section in the Wutaishan/Hengshan/Fuping terrain of northern China. *J. Asian Earth Sci.* (in the press).

Liu, D.Y., Nutman, A. P., Compston, W., Wu, J. S. & Shen, Q.H. Remnants of >3800 Ma crust in the Chinese part of the Sino-Korean craton. *Geology* **20**, 339–342 (1992).

Zhao, G.C., Wilde, S.A., Cawood, P.A. & Sun, M. Archean blocks and their boundaries in the North China Craton: lithological, geochemical, structural and P-T path constraints and tectonic evolution, *Precambr. Res*. **107**, 45–73 (2001).

Supplementary Discussion

A detailed explanation, data sources and modelling parameters for Fig. 4 of Gao et al.

Figure 4 compares Sr-Nd isotopic compositions of the Xinglonggou lavas (this paper) and inferred slab melts from the Aleutians (ref. 15; Yogodzinski & Volynets, 1994; Yogodzinski *et al*., 1995), Baja California (Aguillón-Robles *et al*., 2001), Midanao, Philippines (Sajona *et al*., 2000) and Cook Island, Andean Austral Volcanic Zone (Stern & Kilian, 1996) (open circles; small open circles indicate associated basalts). All isotopic compositions are calculated at 160 Myr. The thick black curves with pluses are AFC (assimilation and fractional crystallization) trends showing 10% increments in F (magma remaining) for a 30% partial melt of the median Xu-Huai eclogite-garnet clinopyroxenite (XH; the large open triangle with 1σ error bars) that assimilates mantle (DM) with the isotopic composition of mid-ocean ridge basalt (MORB). The two trends represent melts derived from xenoliths with the highest (upper curve) and lowest (lower curve) Sr-Nd contents, respectively. The MORB field is from Hofmann (1997); DM composition is from Salters & Stracke (2004). Data for Xu-Huai xenoliths are from Xu *et al*. (ref. 26) and Wang (2003). The depleted eclogitic residue is assumed to consist of 50% garnet and 50% clinopyroxene. The AFC model assumes a ratio of the rate of assimilation to the rate of fractional crystallization (r) close to 1.0 and the reacted mantle to be comprised of 40% garnet, 40% orthopyroxene and 20% clinopyroxene without olivine, in agreement with experimental and empirical studies (ref. 23; Prouteau et al., 2001). However, the presence of olivine has little effect on the results, due to its low partition coefficients for Sr and Nd (similar to those of orthopyroxene) (Fujimaki *et al*., 1984; Dunn & Sen, 1994; Bacon & Druitt, 1998). The trend is not very sensitive to the initial melt composition determined by the degree of partial melting of the median Xu-Huai eclogite-garnet clinopyroxenite, nor to the relative garnet, orthopyroxene and clinopyroxene proportions in the reacted mantle. Initial melt compositions from 10-50% partial melting and a garnet proportion from 10 to 80% also yield trends through the Xinglonggou data, with F ranging from 75 to 90%. The Sr-Nd isotopic compositions of the Xinglonggou lavas are consistent with consumption of <40% melt during reaction with the mantle.

Also shown are AFC and energy-constrained assimilation and fractional crystallization (EC-AFC; Bohrson & Spera, 2001) models for assimilation of slab melt by the North China crust (NCC; average isotopic composition calculated from compilations of Wu *et al*. (in the press) and Sr-Nd elemental concentrations from Gao *et al*., 1998)). The AFC trend (grey broken thin curve with crosses indicating 5% increment in F) passes through the Xinglonggou data only for a very low rate of assimilation (r≤0.15), with less than 20% melt left after assimilation. Using the highest Cr (636 p.p.m.) and Ni (132 p.p.m.) contents in Aleutian high-Mg andesites/adakites (Yogodzinski &Volynets, 1994) as representative of adakite prior to continental crust assimilation, the modelled Cr and Ni in the corresponding melt is <2 p.p.m., which is far lower than observed in the Xinglonggou adakites and andesites (i.e., >120 and >80 p.p.m., respectively, Table 1). Parameters used in the EC-AFC model are given in Supplementary Discussion Table 1. The EC-AFC model uses liquidus temperature and initial temperature of the magma of 1100°C, assimilant liquidus temperature of 1150°C, assimilant initial temperature of 600°C, and assimilant solidus temperature 750°C for an intermediate North China crust (Gao *et al*., 1998). EC-AFC trends (gray thin curves) for equilibration temperatures (T_{eq}) (i.e., the final temperature to which the magma cools and the wallrock heats up) of 800 °C and 755 °C are shown. The EC-AFC trend may pass through the Xinglonggou lavas only when the equilibration temperature is very close to assimilant solidus temperature, with their difference <4°C (not shown for clarity). Such temperatures are considerably lower than the temperature (>800°C) suggested by the presence of orthopyroxene phenocrysts and zircon saturation thermometry (as discussed in text). Moreover, at such temperatures the original melt would have crystallized with minimal assimilation and not erupted. The above modelling indicates that the Xinglonggou lavas did not from via crustal assimilation by a slab melt.

Partition coefficients of Sr between garnet, clinopyroxene and melt are from Klemme *et al.* (2002) and those of Nd are interpolated from values of Pr and Sm (Klemme *et al.,* 2002). Partition coefficients between orthopyroxene and melt are from Bacon & Druitt (1998) and Fujimaki *et al.* (1984) and those between plagioclase and melt from Dunn & Sen (1994).

References not cited in main paper

Aguillón-Robles, A. *et al.* Late Miocene adakites and Nb-enriched basalts from Vizcaino Peninsula, Mexico: Indicators of East Pacific Rise subduction below southern Baja California? *Geology* **29,** 531–534 (2001).

Bacon, C.R. & Druitt, T.H. Compositional evolution of the zoned calc-alkaline magma chamber of Mt. Mazama, Crater Lake, Oregon. *Contrib. Mineral. Petrol.* **98**, 244–256 (1998).

Bohrson, W.A. & Spera, F.J. Energy-constrained open-system magmatic processes II: Application of energy-constrained assimilation-fractional crystallization (EC-AFC) model to magmatic systems. *J. Petrol.* **42**, 1019–1041 (2001).

Dunn, T. & Sen, C. Mineral/matrix partition coefficients for orthopyroxene, plagioclase, and olivine in basaltic to andesitic systems: a combined analytical and experimental study. *Geochim. Cosmochim. Acta* **58**, 717–733 (1994).

Fujimaki, H., Tatsumoto, M. & Aoki, K. Partition coefficients of Hf, Zr, and REE between phenocrysts and groundmass. *Proc.14th Lunar Planet. Sci. Conf. Part 2, J. Geophys. Res.* **89 (suppl)**, 662–672 (1984).

Gao, S. *et al.* Chemical composition of the continental crust as revealed by studies in East China. *Geochim. Cosmochim. Acta* **62,** 1959–1975 (1998).

Hoffmann, A.W. Mantle geochemistry: the message from oceanic volcanism. *Nature* **385,** 219–228 (1997).

Klemme, S., Blundy, J.D. & Wood, B.J. Experimental constraints on major and trace element partitioning during partial melting of eclogite. *Geochim. Cosmochim. Acta* **66,** 3109–3123 (2002).

Prouteau, G., Pichavant, M. & Maury, R.C. Evidence for mantle metasomatism by hydrous silicic melts derived from subducted oceanic crust. *Nature* **410,** 197–200 (2001).

Sajona, F.G. *et al*. Magmatic source enrichment by slab-derived melts in a young post-collision setting, central Mindanao (Philippines). *Lithos* **54**, 173–206 (2000).

Salters, V.J.M. & Stracke, A. Composition of the depleted mantle. *Geochem. Geophys. Geosys*. **5**, Q05004, doi:10.1029/2003GC000597 (2004).

Stern, C.R. & Kilian, R. Role of the subducted slab, mantle wedge and continental crust in the generation of adakites from the Andean Austral Volcanic Zone. *Contrib. Mineral. Petrol.* **123**, 263-281 (1996).

Yogodzinski, G.M. & Volynets, O.N. Magnesian andesites and the subduction component in a strongly calc-alkaline series at Piip Volcano, far Western Aleutians. *J. Petrol.* **35**, 163–204 (1994).

Yogodzinski, G.M., Kay, R.W., Volynets, O.N., Koloskov, A.V. & Kay, S.M. Magnesian andesites in the western Aleutian Komandorsky region: implications for slab melting and metasomatic processes in the mantle wedge. *Geol. Soc. Am. Bull.* **107**, 505–519 (1995).

Wang, H.Q. Petrology and Geochemistry of Mesozoic Intrusive Complex and its Deep-Seated Xenoliths in Xu-Huai region, China: Constraints on Evolution of Mesozoic Lithosphere in Eastern Part of North China Craton. Ph.D. thesis, Jiling University, 145 pp (2003). (In Chinese with English summary).

Wu, F., Zhao, G., Wilde, S.A. & Sun, D. Nd isotopic constraints on crustal formation in the North China Craton. *J. Asian Earth Sci.* (in the press).

Supplementary Discussion Table 1 EC-AFC parameters for Fig. 4_

Thermal parameters		
Magma liquidus temperature $T_{l,m}$	1100	°C
Magma initial temperature T_m^0	1100	°C
Assimilant liquidus temperature $T_{l,a}$	1150	°C
Assimilant initial temperature T_a^0	600	°C
Assimilant solidus temperature T_s	750	°C
Equilibration temperature T_{eq}	800, 755	°C
Crystallization enthalpy Δh_{cry}	357941	J/kg
Isobaric specific heat of magma $C_{p,m}$	1423	J/kg per K
Fusion enthalpy Δh_{fus}	381848	J/kg
Isobaric specific heat of assimilant $C_{p,a}$	1409	J/kg per K
Compositional parameters	Sr	Nd
Magma initial concentration (p.p.m.) C_m^0	502	10.7
Magma isotope ratio ε_m	0.702725	0.512866
Magma trace element distribution coefficient D_m	1.027	0.128
Assimilant initial concentration (p.p.m.) C_a^0	336	25
Assimilant isotope ratio ε_a	0.714855	0.511178
Assimilant trace element distribution coefficient D_a	1.027	0.128